# HIF1α Induces the Recruitment of Bone Marrow-Derived Vascular Modulatory Cells to Regulate Tumor Angiogenesis and Invasion

Rose Du,[1,7,10] Kan V. Lu,[1,10] Claudia Petritsch,[1] Patty Liu,[1] Ruth Ganss,[8] Emmanuelle Passegué,[2] Hanqiu Song,[1] Scott VandenBerg,[1,3] Randall S. Johnson,[9] Zena Werb,[4,6] and Gabriele Bergers[1,5,6,*]

[1]Department of Neurological Surgery
[2]Department of Developmental and Stem Cell Biology
[3]Department of Pathology
[4]Department of Anatomy
[5]Brain Tumor Research Center
[6]UCSF Helen Diller Family Comprehensive Cancer Center
University of California, San Francisco, 513 Parnassus Avenue, San Francisco, CA 94143, USA
[7]Department of Neurological Surgery, Brigham and Women's Hospital, Harvard Medical School, 75 Francis Street, Boston, MA 02115, USA
[8]Western Australian Institute for Medical Research, Perth WA 6000, Australia
[9]Molecular Biology Section, Division of Biological Sciences, University of California, San Diego, La Jolla, CA 92093, USA
[10]These authors contributed equally to this work.
*Correspondence: gabriele.bergers@ucsf.edu
DOI 10.1016/j.ccr.2008.01.034

## SUMMARY

Development of hypoxic regions is an indicator of poor prognosis in many tumors. Here, we demonstrate that HIF1α, the direct effector of hypoxia, partly through increases in SDF1α, induces recruitment of bone marrow-derived CD45+ myeloid cells containing Tie2+, VEGFR1+, CD11b+, and F4/80+ subpopulations, as well as endothelial and pericyte progenitor cells to promote neovascularization in glioblastoma. MMP-9 activity of bone marrow-derived CD45+ cells is essential and sufficient to initiate angiogenesis by increasing VEGF bioavailability. In the absence of HIF1α, SDF1α levels decrease, and fewer BM-derived cells are recruited to the tumors, decreasing MMP-9 and mobilization of VEGF. VEGF also directly regulates tumor cell invasiveness. When VEGF activity is impaired, tumor cells invade deep into the brain in the perivascular compartment.

## INTRODUCTION

When tumors encounter low oxygen tension, they adapt by promoting expression of genes associated with anaerobic cell metabolism, cell survival, angiogenesis, metastasis and invasion. This transcriptional response pathway is mediated to a large extent by the dimeric transcription factor complexes of hypoxia-inducible factor HIF1 and HIF2 (Giaccia et al., 2004; Lofstedt et al., 2007). At normoxia, HIFα subunits are degraded, but they are stabilized and activated under hypoxic conditions and form complexes with the constitutively expressed transcription factor ARNT/HIF1β (Giaccia et al., 2004; Lofstedt et al., 2007).

Congruent with the observation that poor oxygenation, concomitant with HIF1α induction, is associated with a more aggressive tumor phenotype, genetic ablation of HIF1α in various tumors results in reduced tumor mass, increased apoptosis, and retarded metastasis due in part to reduced vascular density and inhibition of angiogenesis (Maxwell et al., 1997; Ryan et al., 1998; Liao et al., 2007; Blouw et al., 2003). HIF1 activity

stimulates neovascularization by enabling tumor and host cells to produce a variety of proangiogenic factors like VEGF-A, VEGFR1, PDGF-B, FGF-2, and angiopoietins that stimulate new blood vessel formation within hypoxic areas (Shweiki et al., 1992) (Calvani et al., 2006; Holash et al., 1999; Okuyama et al., 2006).

New blood vessel formation in tumors and ischemic tissues is derived from the existing vasculature by activating proliferation and migration of endothelial cells (angiogenesis) and recruiting a heterogeneous population of bone-marrow-derived cells (BMDCs), including endothelial progenitor cells (EPC), pericyte progenitor cells (PPC), and CD45+ vascular modulatory cells (Aghi and Chiocca, 2005; De Palma et al., 2005; Grunewald et al., 2006; Heissig et al., 2002; Kopp et al., 2006; Lin et al., 2006; Lyden et al., 2001; Pollard, 2004; Rafii et al., 2002; Rajantie et al., 2004; Song et al., 2005). While EPCs incorporate into the vasculature and differentiate into endothelial cells, PPCs envelop blood vessels and mature into pericytes and vascular smooth muscle cells.

CD45+ cells of monocytic lineage make up the largest and most heterogeneous group of BMDCs that function as vascular modulators, but are not physically part of the vasculature (Grunewald et al., 2006). Such cells include tumor-associated macrophages (TAMs) (Pollard, 2004) and immature monocytic cells including Tie2+ monocytes (TEMs) (De Palma et al., 2005), VEGFR1+ hemangiocytes (Hattori et al., 2002), and CD11b+ myeloid cells (Yang et al., 2004), all of which express the receptor CXCR4 to some extent. Little is known about the factors that enable the mobilization of BMDC from the bone marrow into the blood stream and their recruitment and retention into the tumor. The most prominent factors identified thus far include VEGF, angiopoietin-1, PlGF and PDGF-B, which mobilize EPCs and PPCs, respectively (Hattori et al., 2001; Li et al., 2006; Rabbany et al., 2003; Gerhardt and Betsholtz, 2003), and SDF1$\alpha$, which can facilitate CXCR4+ BMDC retention within tumors (Grunewald et al., 2006; Hattori et al., 2003). Supported by recent data that ischemic tissues may recruit endothelial progenitors and other CXCR4+ BMDCs, in part through increases in HIF and its targets SDF1$\alpha$ and VEGF (Aghi et al., 2006; Ceradini et al., 2004; De Falco et al., 2004; Petit et al., 2007), here we test the hypothesis that hypoxic conditions in tumors as well as in normal tissues promote neovascularization in a HIF-dependent manner by mediating BMDC recruitment.

We assessed this hypothesis in an orthotopic mouse model of glioblastoma (GBM, grade IV astrocytoma) because these aggressive brain tumors are very hypoxic and highly angiogenic (Zagzag et al., 2000), and loss of HIF1$\alpha$ activity in these tumors blocks vascular remodeling and angiogenesis (Blouw et al., 2003). We found that while tumor vessels in GBM are hyperdilated, distorted, and leaky, tumor vessels in HIF-deficient (HIFko) GBM remain slim and regularly shaped and are more reflective of normal brain vasculature. HIFko GBM, however, adapt to their inability to form new vessels by co-opting and moving along blood vessels, a phenomenon defined as perivascular invasion, hence becoming more invasive (Blouw et al., 2003). In the present study, we inquired about the mechanisms by which HIF1$\alpha$ stimulates vascular remodeling and angiogenesis and blocks the perivascular invasive evasive adaptation mechanism.

## RESULTS

### HIF1 Recruits Bone Marrow-Derived Cells to the Tumor Site

To test the hypothesis that GBMs promote BMDC-dependent neovascularization in a HIF-dependent manner, we transplanted bone marrow cells from $\beta$-actin-EGFP mice into lethally irradiated Rag1-deficient (Ragko) mice. Four weeks later, mice were implanted intracranially with HIF1$\alpha$-proficient (WT-GBM) or HIF1$\alpha$-deficient (HIFko GBM) GBM cells. We found that GFP+ BMDCs were randomly distributed within the tumor and represented about 15%–20% of all cells in WT-GBM tumors, whereas HIFko GBMs contained only about one-third this number (Figure 1A). Normal brain recruited virtually no GFP+ cells. These results indicate that HIF1$\alpha$ activity promotes recruitment of a substantial number of BMDCs in GBM.

We next assessed the BMDC types recruited by HIF1 by fluorescence-activated cell sorting (FACS) and immunohistochemical analyses of the tumor-derived GFP+ cell populations. WT-GBM elicited about three times more CD45^{+} monocytic cells and seven times more PDGFR$\beta$[+]/Sca-1^{+} PPCs than HIFko GBM (Figure 1B). WT-GBM also contained nearly four times as many EPCs as HIFko GBM (Figure 1B). Importantly, GFP+ BMDCs were comprised of about 8% EPCs and 2% PPCs, respectively, while up to 90% (about 16% of total cells within the tumor) were positive for the panleukocyte marker CD45 (Figure 1B). The majority of the CD45+ BMDCs were reminiscent of CD11b^{+} monocytes/myeloid cells and F4/80^{+} macrophages, with ∼5% comprised of Tie2^{+} expressing monocytes or VEGFR1+ hemangiocytes (Figure 1C). All CD45+ subpopulations were reduced 2- to 4-fold in HIFko GBM. These results indicate that HIF1 activation results in recruitment of heterogeneous populations of BMDC. Given that all of these cell types are diminished in HIFko GBM, our data suggest that a reduction in the number of BMDCs may be the limiting factor in promoting angiogenesis.

### HIF1 Induces SDF1$\alpha$ in Tumor Cells

This result raises the question about the signaling events that recruit BMDC in a HIF-dependent manner. Both VEGF, which is implicated in the recruitment of vascular progenitor cells (Hattori et al., 2001), and stromal-derived factor 1$\alpha$ (SDF1$\alpha$/CXCL12), which signals through CXCR4 and may retain CXCR4+ BMDC in tumors (Grunewald et al., 2006; Hattori et al., 2003), are HIF1 target genes (Ceradini et al., 2004; Shweiki et al., 1992). Indeed, WT-GBM produced about 4-fold higher levels of VEGF and SDF1$\alpha$ than HIFko GBM (Figure 1D). While WT-GBM contained clusters of SDF1$\alpha$+ cells, HIFko GBM contained only few single SDF1$\alpha$+ cells within tumors (Figure 1E). Importantly, we found that WT-GBM cells, but not HIFko GBM cells, upregulated SDF1$\alpha$ mRNA under hypoxic conditions (Figure 1F), implying that GBMs, through HIF1 and its target SDF1$\alpha$, recruit CXCR4+ BMDCs to the tumor site to facilitate new blood vessel growth.

### HIF1 Recruits MMP-9-Positive Monocytic Cells from the Bone Marrow

If HIF1-induced BMDC influx regulates neovascularization, then which of the BMDC are functionally significant in this process
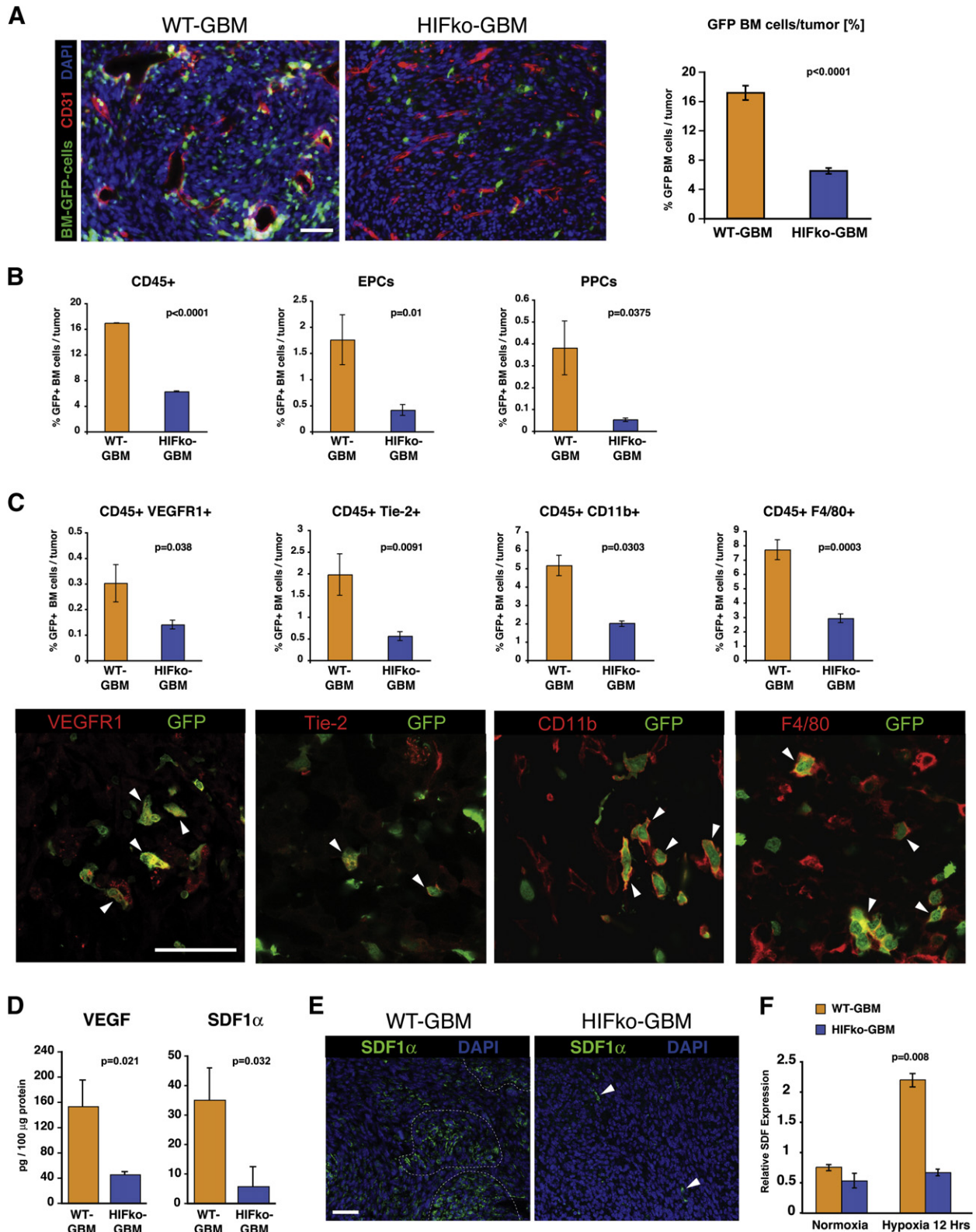
**Figure 1. HIF1 Recruits Bone Marrow-Derived Cells to Orthotopic Glioblastomas**

(A) Immunofluorescent analysis of GBM tumors. HIFko GBM contained ~4 times less GFP+ BMDCs (green) than WT-GBM (n = 4 to 5 fields per tumor of 7 tumors/group). Angiogenic vasculature (red) in WT-GBMs was tortuous, hyperdilated, and distorted, whereas vessels in nonangiogenic HIFko GBMs appeared slim and more regular. Scale bar, 50 μm.

and how do they achieve angiogenic initiation in GBM? Clearly, EPCs and PPCs could support new vessel formation by providing an additional source of endothelial cells and pericytes (Kopp et al., 2006; Rajantie et al., 2004; Song et al., 2005). However, it is less obvious what roles the heterogeneous CD45+ myeloid cell populations play. Therefore, we used a candidate approach to identify proangiogenic molecules produced or regulated by vascular-modulating CD45+ BMDCs. Recent studies have shown that these cells express matrix metalloproteinase (MMP)-9 (Jodele et al., 2005; Page-McCaw et al., 2007; Yang et al., 2004; Nozawa et al., 2006). We had discovered that MMP-9, conveyed by inflammatory cells, enables an angiogenic switch by making sequestered VEGF bioavailable for its receptor VEGFR2 in pancreatic islet tumors (Bergers et al., 2000; Nozawa et al., 2006). In human astrocytomas, MMP-9 expressed in inflammatory cells and the invading tumor cell compartment correlates with tumor progression (Hormigo et al., 2006; Kunishio et al., 2003). We observed that the expression of MMP-9 in GBM was substantially reduced in the absence of HIF1 (Figure 2A). Similar to human GBMs, WT-GBM expressed MMP-9 in monocytic cells including F4/80+ macrophages and Tie2+, CD11b+, and VEGFR1+ myeloid populations (Figure 2B). We also detected MMP-9 in a small subset of tumor cells within the tumor mass and in single tumor cells infiltrating the brain parenchyma, as visualized by double positivity for SV40Tag and MMP-9, which were diminished in HIFko GBMs (Figure 2C). Substrate-gel zymography revealed that most of MMP-9 in the tumors was in an active form and reduced in HIFko GBM (Figure 2D).

Given that HIFko GBM do not undergo vascular remodeling, we hypothesized that the nonangiogenic behavior of HIFko GBM is mainly caused by the substantial reduction of MMP-9-expressing BMDCs in the tumors. The reduced levels of MMP-9 would then keep VEGF in a predominantly sequestered state. Indeed, when we ectopically expressed active MMP-9 in HIFko-GBM cells (HIFko MMP-9+) to increase intratumoral MMP-9 levels (Figure 2E), tumors became hemorrhagic (Figure 2F) and, to a certain extent, exhibited a tortuous, irregularly shaped and hyperdilated vasculature indicative of vascular remodeling (Figure 2G), keeping with the observation that an early indication of VEGF activity is vascular hyperdilation (Dvorak, 2000). Since the VEGF levels in HIFko GBM are about 3.5-fold less than in WT-GBM (Figure 1D), the magnitude of these responses would be expected to be limited due to the rather low VEGF levels. Thus, although VEGF is liberated from the matrix in the presence of MMP-9, the total VEGF levels are not sufficient to produce the vigorous angiogenesis seen in WT-GBM. Indeed, we confirmed that the soluble VEGF fraction was substantially higher in HIFko MMP-9+ GBM compared to mock transfectants (Figure 2H). Our data suggest that HIF1 regulates two steps of VEGF activity: it both induces VEGF levels and regulates its mobilization from the ECM by recruiting monocytes that transport MMP-9 to the tumor site.

## MMP-9 Deficiency Impedes Vascular Remodeling and Neovascularization in GBM

If MMP-9 is a critical downstream factor of HIF1α regulating angiogenesis, then MMP-9 deficiency should give rise to tumors that, like HIFko GBMs, are nonangiogenic. We, therefore, generated MMP-9ko GBMs in the same manner we produced WT-GBM and HIFko GBMs (Blouw et al., 2003). Both MMP-9ko GBM and WT-GBM cells gave rise to similar numbers of soft agar colonies (Figure S1). MMP-9ko GBMs injected into MMP-9ko mice exhibited typical features of high-grade astrocytomas/GBMs, and although they did not differ from WT-GBM in proliferation, these mice exhibited modestly longer survival times than wild-type mice bearing WT-GBM (Figure S1).

We found that the majority of tumor vessels from MMP-9ko tumors were slim, elongated, and regularly shaped as visualized by fluorescent angiography, similar to blood vessels in normal brain, and in contrast to the distorted and angiogenic tumor vasculature from WT-GBM (Figure 3A). Congruent with the morphologic changes of an angiogenic tumor vasculature, we observed VEGF-VEGFR2-complex formation, which marks the activated, angiogenic state on endothelial cells (Bergers et al., 2000; Brekken et al., 2000) (Figure 3C), and RGS-5 expression (Figure 3D), a marker of activated pericytes (Berger et al., 2005; Bondjers et al., 2003), in WT-GBMs but not in MMP-9ko tumors (Figures 3C and 3D). These results indicate that tumor vessels in the absence of MMP-9 did not undergo vascular remodeling.

Notably, the inability of VEGF to bind to its receptor in MMP-9ko tumors was not caused by a severe reduction in VEGF or its receptor VEGFR2 (Figures 3B and 3E) because VEGF levels were comparable to those of WT-GBM (Figure S2). However, most of the VEGF-164, the predominant VEGF isoform in GBM, was bound to the extracellular matrix and cell surface of MMP-9ko tumor cells and, unlike WT-GBM, was not present in the supernatant (Figures 3F and 3G). These data confirm our observation in HIFko MMP-9+ tumors that MMP-9 is an important initiator of angiogenesis in GBM by releasing sequestered VEGF and making it bioavailable to its receptor VEGFR2.

## Bone Marrow-Derived MMP-9+ Cells Are Sufficient to Initiate the Angiogenic Switch in GBM

To determine whether MMP-9 in tumor cells or host cells is critical for the angiogenic phenotype, we implanted WT-GBM cells into MMP-9ko mice (Figure 4A), and MMP-9ko GBMs into

(B) Fluorescence-activated cell sorting (FACS) analysis of GBM tumors. HIF1 recruited three distinct GFP+ BMDC populations to the tumor site: CD45+ monocytes, endothelial progenitors (EPC) (VE-Cadherin+/VEGFR2+), and pericyte progenitors (PPC) (Sca1+/PDGFRβ+) (n = 4 to 5/group). Error bars indicate ± SEM.
(C) FACS and immunohistochemical analyses. Subsets of the GFP+ BMDC population of CD45+ monocytes were VEGFR1+, Tie2+, CD11b+ myeloid cells, and F4/80+ macrophages (all labeled in red, white arrowheads). Scale bar, 50 μm. All CD45+ subpopulations were reduced 2- to 4-fold in HIFko GBM. (n = 3 to 4/group). Error bars indicate ± SEM.
(D) ELISA assay. Intratumoral VEGF and SDF1α was ∼4 times higher in WT-GBM than HIFko GBM (n = 3 to 4/group).
(E) Immunohistochemical analysis of SDF1α. WT-GBM contained clusters of SDF1α+ cells (green, encircled), whereas SDF1α expression in HIFko GBM was limited to a few single cells (white arrows). Scale bar, 50 μm.
(F) Real-time PCR analysis. HIF1 induced SDF1α in GBM tumor cells. WT-GBM and HIFko GBM cells were cultured under normoxic (20% pO$_2$) or hypoxic conditions (1% pO$_2$) for 12 hr and harvested, and transcription levels of SDF1α were determined. Error bars indicate ± SEM.
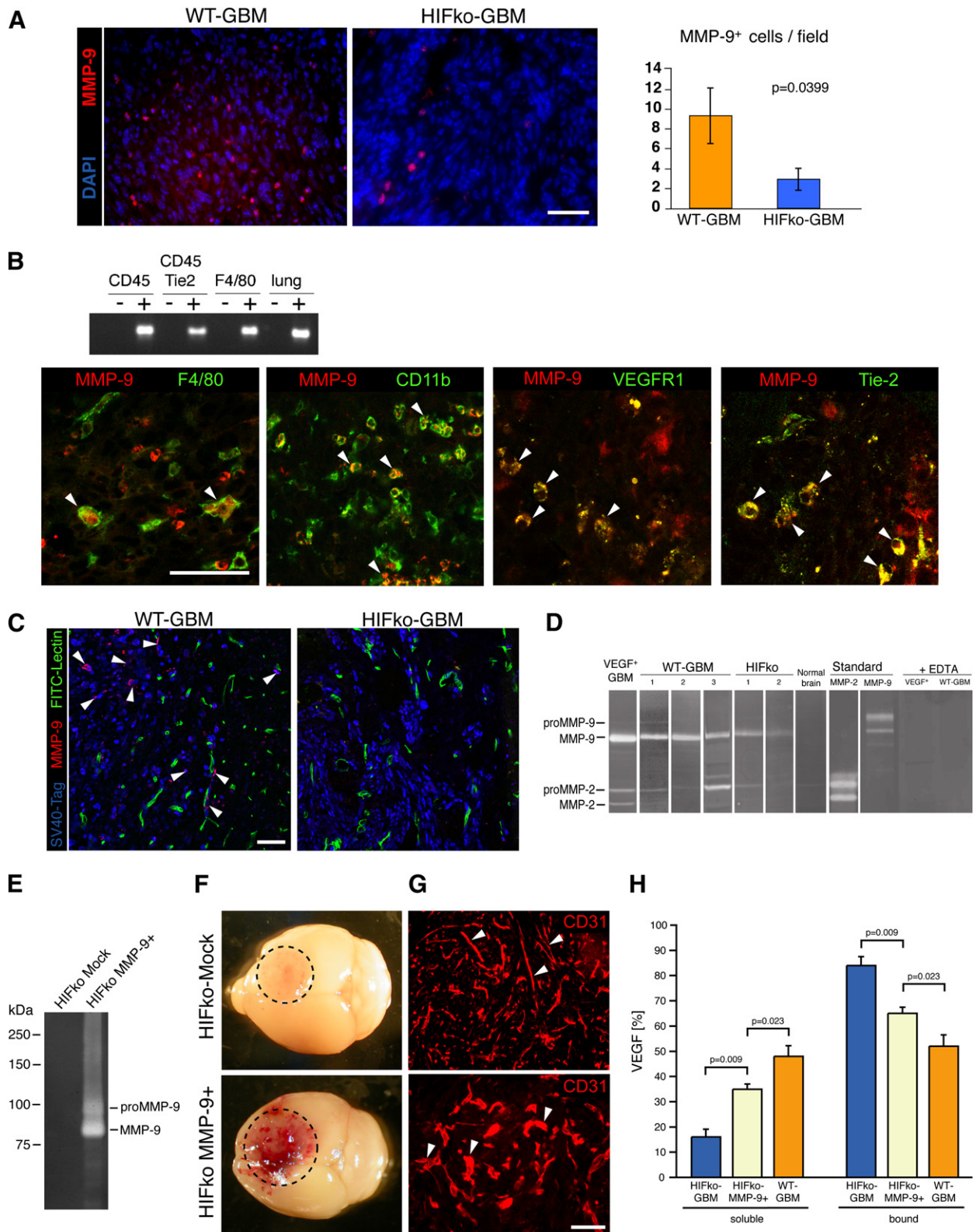
**Figure 2. MMP-9 Is Expressed in Various Subpopulations of CD45+ BMDC and in Infiltrating Tumor Cells**

(A) Immunohistochemical analysis. WT-GBMs contained about 3.5 times more MMP-9+ cells than HIFko GBMs (n = 4 fields per tumor of 5 tumors/group). Scale bar, 50 μm. Error bars indicate ± SEM.
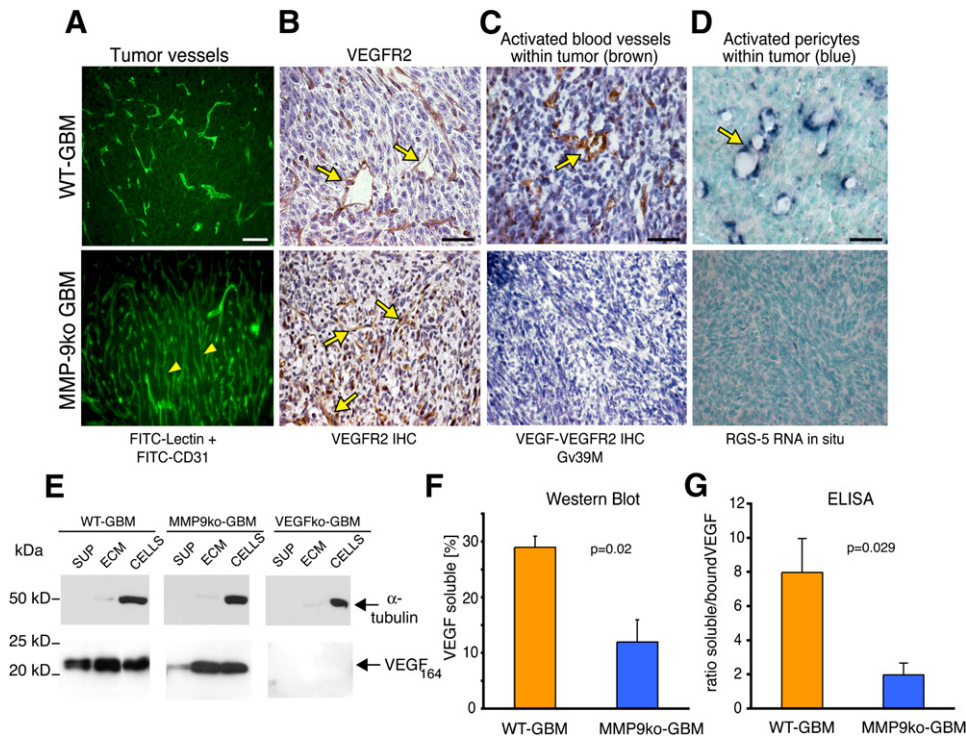
**Figure 3. MMP-9-Deficient GBM Do Not Undergo Vascular Remodeling and Neovascularization**

(A) FITC-lectin perfusion of the tumor vasculature and anti-CD31 immunohistochemical analysis (green). In the complete absence of MMP-9, tumor vessels did not undergo vascular remodeling but contained a regular, slim, and dense vascular network (yellow arrowheads). All scale bars, 50 μm.
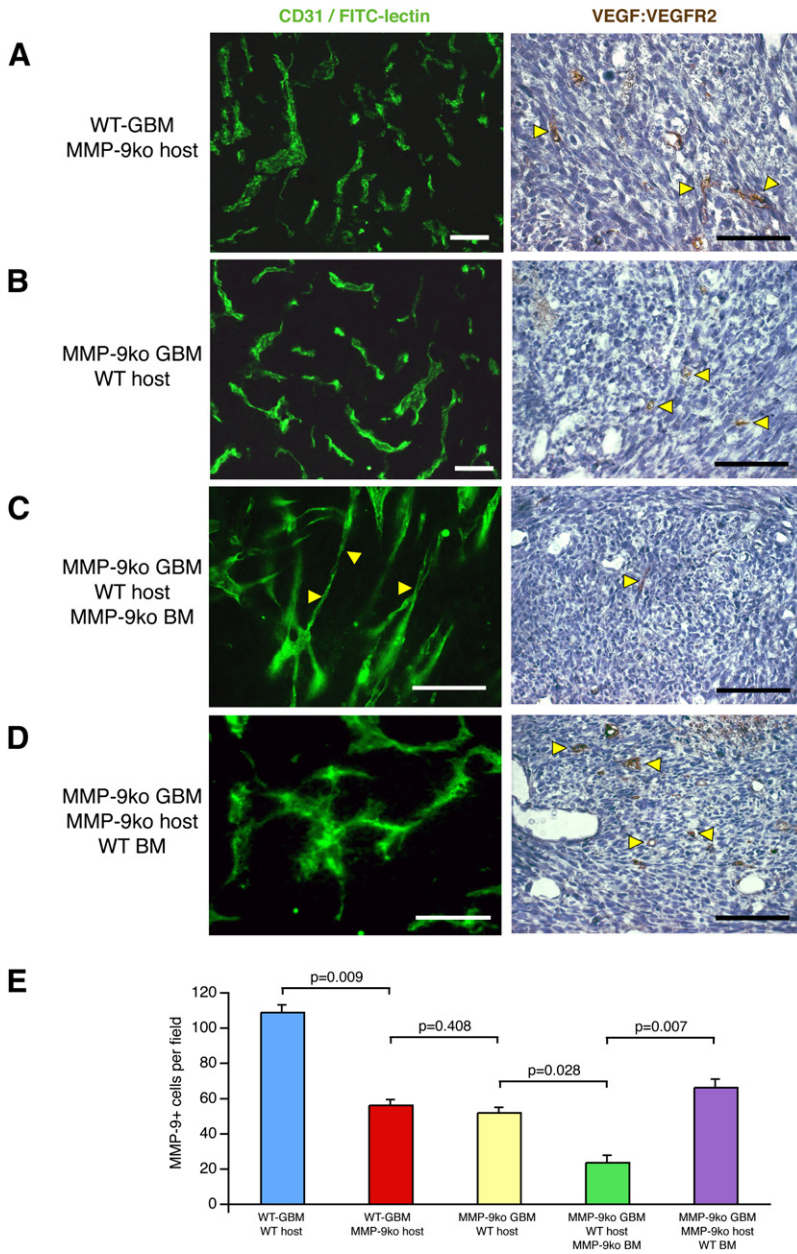
(B) Immunohistochemical analysis. VEGFR2 expression on tumor endothelial cells was apparent in WT-GBM and MMP-9ko GBM (yellow arrows).

(C) Immunohistochemical analysis. Activated tumor vessels were detected with the Gv39M antibody that recognizes the VEGF:VEGFR2 complex (brown) in WT-GBM, but not in MMP-9ko tumors.

(D) In situ RNA hybridization. RGS-5 (blue), a marker for activated pericytes, was expressed in pericytes of WT-GBM, but not in MMP-9ko GBM.

(E) VEGF western blot analysis of tumor cells. In WT-GBM, soluble VEGF was detected in the supernatant of GBM. In MMP-9ko GBM, VEGF-164 was predominantly sequestered in the ECM and bound to cell surfaces. VEGFko GBM served as negative controls.

(F) Quantification of soluble VEGF levels determined by densitometry of VEGF western blots shown in (E). Soluble VEGF was significantly decreased in the absence of MMP-9. Error bars indicate SEM.

(G) ELISA. Ratio of soluble VEGF (in supernatant) and sequestered VEGF (ECM and cells) was determined in WT-GBM and MMP-9ko GBM. Soluble, mobilized VEGF was significantly reduced in MMP-9ko GBM. Error bars indicate SEM.

wild-type (WT) hosts (Figure 4B). In both instances, tumor vessels were irregularly shaped and tortuous indicative of vascular remodeling and showed VEGF/VEGFR2 binding, albeit to a lesser extent than WT-GBM in WT hosts, indicating that as long as a critical threshold of MMP-9 exists in tumors, angiogenesis can be initiated. In both instances, MMP-9+ cell numbers were reduced by 50% when compared to the WT situation (Figure 4E). Interestingly, when we injected MMP-9ko GBMs into WT mice

whose bone marrow was reconstituted with MMP-9ko bone marrow, MMP-9+ cells in the tumors dropped significantly by 3- to 4-fold compared to WT-GBM, while blood vessels were more elongated and slim and did not exhibit VEGF:VEGFR2 activation, mimicking the phenotype of MMP-9ko tumor blood vessels in a MMP-9ko host (Figures 4C and 4E). Similarly, when we reconstituted the bone marrow of MMP-9ko mice harboring MMP-9ko GBM with WT bone marrow, the number

(B) RT-PCR analyses of fractionated cell populations from the tumor and immunohistochemical analyses. MMP-9 was expressed in F4/80+ macrophages, CD11b+ myeloid cells, VEGFR1+ hemangiocytes, and in Tie2+ monocytes. Scale bar, 50 μm.

(C) MMP-9 was expressed in a small subset of tumor cells at the invading edge of WT-GBM, but not in the perivascular invasive areas of HIFko GBMs. (MMP-9+ cells, red; SV40Tag+ tumor cells, blue; blood vessels, green). Scale bar, 50 μm.

(D) Gelatin zymography. WT-GBM tumors contained predominantly active MMP-9 and, to a much lesser extent, MMP-2. In HIFko GBM, MMP-9 activity was reduced. As controls, recombinant pro-MMP-9 and -2 as well as active MMP-9 and -2 were loaded, and MMP-activity was obliterated in the presence of the MMP-inhibitor EDTA.

(E) Gelatin zymography. HIFko MMP-9+ cells that ectopically express MMP-9 had substantially higher MMP-9 activity than mock-infected control.

(F) HIFko MMP-9+ GBM, but not HIFko Mock control tumors, were hemorrhagic by gross morphology.

(G) Blood vessels in HIFko Mock control tumors were slim and elongated, whereas vessels in HIFko MMP-9+ tumors were rather distorted and hyperdilated.

(H) ELISA assay. Soluble VEGF was measured in GBM in the supernatant. Sequestered (bound) VEGF was determined both in the ECM and in GBM cells. Error bars indicate SEM.

**Figure 4. MMP-9+ BMDCs Contribute to the Angiogenic Switch in GBM**

Immunohistochemical analysis and FITC-lectin perfusion of mice (A–D). The activated tumor vasculature was identified by the presence of VEGF:VEGFR2 complexes on endothelial cells. Cohorts of 6–13 mice were used. White bars, 50 μm. Black bars, 75 μm.

(A) WT-GBM cells in MMP-9ko mice. Vascular remodeling of tumor vessels was indicated by their irregular shape and the presence of a few activated tumor vessels (yellow arrowheads).

(B) MMP-9ko GBM cells in wild-type mice. Vascular remodeling of tumor vessels was indicated by their irregular shape and the presence of a few activated tumor vessels (yellow arrowheads).

(C) Wild-type mice, reconstituted with MMP-9ko bone marrow, were injected with MMP-9ko GBM cells. Tumor vessels contained areas of elongated and slim vessels mimicking the phenotype of MMP-9ko tumor vessels and did not exhibit VEGF:VEGFR2 activation on tumor endothelial cells.

(D) MMP-9ko mice, reconstituted with wild-type bone marrow, were injected with MMP-9ko GBM cells. Tumor vessels appeared torturous, hyperdilated, and irregularly shaped, concomitant with VEGF:VEGFR2 activation on tumor endothelial cells.

(E) The number of MMP-9+ cells correlated with the angiogenic phenotype of the tumors described in (A)–(D). Error bars indicate SEM.

GFP bone marrow cells revealed a 4-fold reduction of VEGFR2+ GFP+ EPC incorporated into tumor vessels when compared to WT-GBM (Figure 5A). Using two different pericyte markers (desmin and α-smooth muscle actin [α−SMA]) to detect pericytes (Figure 5B), we also observed about 50% less pericyte coverage in the absence of MMP-9. Upon transplantation of MMP-9ko GBM-bearing MMP-9ko mice with WT bone marrow, pericyte coverage increased, approximating the WT situation (Figure 5B). In contrast, when we reconstituted bone marrow of WT tumor-bearing mice with MMP-9ko bone marrow, we lowered pericyte coverage, indicating that a subpopulation of pericytes is recruited from the bone marrow in a MMP-9-dependent manner (Figure 5B).

of MMP-9+ cells increased while blood vessels became enlarged and distorted, exhibiting typical features of vascular remodeling concomitant with VEGF binding to its receptor (Figures 4D and 4E).

These data support the notion that a specific MMP-9 threshold is required for the angiogenic switch and that, indeed, BMDCs expressing MMP-9 have a significant effect on GBM angiogenesis.

## MMP-9 Enables Recruitment of EPC and PPC to the GBM Vasculature

To elucidate how MMP-9+ BMDCs promote GBM angiogenesis, we analyzed whether lack of MMP-9 in bone marrow cells impacts recruitment of vascular progenitor cells and CD45+ myeloid vascular support cells. Transplant experiments with actin-

## Recruitment of CD45+ Cells Is Independent of MMP-9 but Dependent on SDF1α

We then asked whether MMP-9 is also required for recruitment of the CD45+ population of BMDC in GBM. We observed similar numbers of CD45+ cells in MMP-9ko GBM and WT-GBM tumors (Figure 5C). By contrast, we observed an ∼3-fold reduction in the number of CD45+ and F4/80+ cells in HIFko GBMs when compared to WT tumors (Figure 5C). Similarly, while WT-GBM and MMP-9ko GBM expressed comparable levels of SDF1α, HIFko GBM expressed severely reduced levels of SDF1α, reflective of the differing CD45+ cell influx in the respective tumors (Figure 5C). These data suggest that GBMs recruit CXCR4+

BMDC to the tumor site through HIF1 and its target SDF1α to facilitate new blood vessel growth.

To demonstrate the functional significance of SDF1α in neovascularization, we treated WT-GBM bearing mice with the CXCR4 inhibitor AMD3100 (Petit et al., 2007). AMD3100 substantially reduced the recruitment of CXCR4+/CD45+ BMDC (Figure 5D), and tumor vessels appeared slimmer and "normalized" as observed when angiogenesis is inhibited (Figure 5E).

## BMD-CD45+ Cells Are Sufficient to Initiate Neovascularization in GBM

Since AMD3100 also blocks CXCR4+ EPC, we sought to investigate whether the CXCR4+ monocytic population is functionally significant and sufficient in promoting the angiogenic switch. While both EPC and PPC populations were reduced in MMP-9ko GBM, we found that MMP-9ko GBM and WT-GBM contained similar numbers of CD45+ BMDC (Figure 5C), indicating that recruitment of these monocytic cells is independent of MMP-9 in the bone marrow. This suggested that MMP-9ko tumors were nonangiogenic, despite the unaltered levels of monocytic cells, because CD45+ cells lacked MMP-9 necessary to initiate neovascularization, whereas HIFko tumors were nonangiogenic because they had reduced numbers of CD45+ cells and, thus, insufficient MMP-9 to commence neovascularization. To assess the functional significance of MMP-9+ CD45 cells in this process, we isolated MMP-9-proficient GFP+ CD45+ cells from bone marrow of WT mice and injected them intravenously into MMP-9ko mice bearing MMP-9ko GBM (Figure 5F). We used MMP-9ko GFP+ CD45+ cells as controls. We confirmed by zymogram analysis that injections of MMP-9+ CD45+ cells led to MMP-9 activity in the tumor, whereas injection of MMP-9ko CD45+ cells did not (Figure 5G), and that tumors recruited GFP+ CD45+ MMP-9-proficient or -deficient cells at similar levels (Figure 5H). The tumors that attracted CD45+ MMP-9+ BMDC exhibited hyperdilated and more irregularly shaped vessels, whereas GBM that attracted CD45+ MMP-9ko cells did not alter their slim vascular anatomy (Figures 5I and 5J). Notably, we often detected MMP-9+ cells encircling enlarged tumor vessels (Figure 5J), suggesting that MMP-9 may preferentially facilitate local "activation" of sequestered VEGF. We further noticed that VEGFR2 activation occurred in tumors undergoing vascular remodeling, but not in tumors that received CD45+MMP-9ko cells (Figure 5K). Taken together with the results in Figures 3 and 4, these data reveal that MMP-9 expressed and secreted by a heterogeneous group of CD45+ cells from the bone marrow is sufficient to initiate angiogenesis by making sequestered VEGF bioavailable to its receptor VEGFR2.

## VEGF Is a Direct and Negative Regulator of Perivascular Tumor Invasion

In view of our previous observation that genetic ablation of HIF1α or VEGF (Blouw et al., 2003), which blocks the ability of GBM to initiate VEGF-dependent neovascularization, results in a more invasive phenotype, we reevaluated the paradigm of angiogenesis as being key to tumor progression. It is important to note that the induced invasive mode in the absence of these angiogenic factors was distinct from the invasive mode in WT-GBM because tumor cells predominantly moved along blood vessels in the brain parenchyma (Blouw et al., 2003; present paper;

Figure 6A white arrows). In contrast, WT-GBMs have a more infiltrative behavior in which tumor cells percolate as single cells through the brain parenchyma (Figure 6A, yellow arrows). Interestingly, we found that MMP-9 was expressed in a subset of these infiltrating cells, while MMP-9 was not detected in HIFko GBMs migrating along blood vessels (Figure 2C). These data support the hypothesis that MMP-9 facilitates infiltration of tumor cells directly but is not implicated in the perivascular invasive mode. Because MMP-9ko GBMs do not undergo vascular remodeling, we predicted that they would display a more perivascular invasive phenotype. We observed that GBM in the complete absence of MMP-9 grew more diffusely into the brain parenchyma than WT-GBM (Figure 6A). Notably, while WT-GBMs in a WT host and WT-GBMs in an MMP-9ko host both preferentially infiltrated into the brain parenchyma, loss of MMP-9 in the tumor cell compartment alone was sufficient to tip the balance to a more perivascular invasive mode, which was even more exaggerated in the complete absence of MMP-9 and comparable to the phenotype observed in HIFko GBM tumors (Figure 6B). Notably, regardless of whether HIF1α or MMP9 was completely ablated, disabling angiogenesis resulted in a perivascular invasive phenotype.

These results point to a specific adaptation mechanism for GBM when deprived of key angiogenic factors that drive VEGF-dependent neovascularization and suggest that the mechanisms of tumor cell infiltration and perivascular tumor cell invasion are very distinct. Since perivascular tumor invasion is negatively correlated with angiogenesis, we then tested the hypothesis that VEGF is the negative regulatory factor. Indeed, by ectopically expressing VEGF-164, the major VEGF isoform expressed in GBM, we were able to convert HIFko GBMs, which are highly invasive and produce low levels of VEGF, into noninvasive tumors with smooth borders (Figure 6C).

How does VEGF-induced angiogenesis block perivascular invasion? Based on several reports that tumor cells can express VEGF receptors (Lesslie et al., 2006), we asked whether VEGF has a direct effect on the invasive behavior of GBM. Both WT-GBM and HIFko GBM cell lines expressed VEGFR1 and -2 receptors to varying extents, as well as the coreceptors neuropilin-1 (NP-1) and neuropilin-2 (NP-2) (Figure 6D). We then tested the ability of VEGF to affect invasive behavior of GBM cells directly in vitro in a Boyden chamber assay. Both WT-GBM and HIFko GBM cells were highly invasive in response to HGF, a stimulator of GBM invasion (Abounader and Laterra, 2005; Eckerich et al., 2007), but surprisingly, VEGF reduced their invasive behavior significantly (Figure 6F). Similarly, HIFko GBM cells overexpressing VEGF were less invasive than their parental counterparts (Figure 6E). VEGF alone did not stimulate or inhibit invasiveness of GBM cells. In summary, these results reveal that VEGF acts as a direct negative regulator of perivascular GBM tumor cell invasion.

## DISCUSSION

### HIF1 Is a Key Regulator for BMDC Recruitment in Tumors

In this study, we have demonstrated that HIF1, in part by inducing SDF1α, is a major recruitment regulator of bone marrow-derived EPC, PPC, and monocytic vascular modulatory cells to endorse
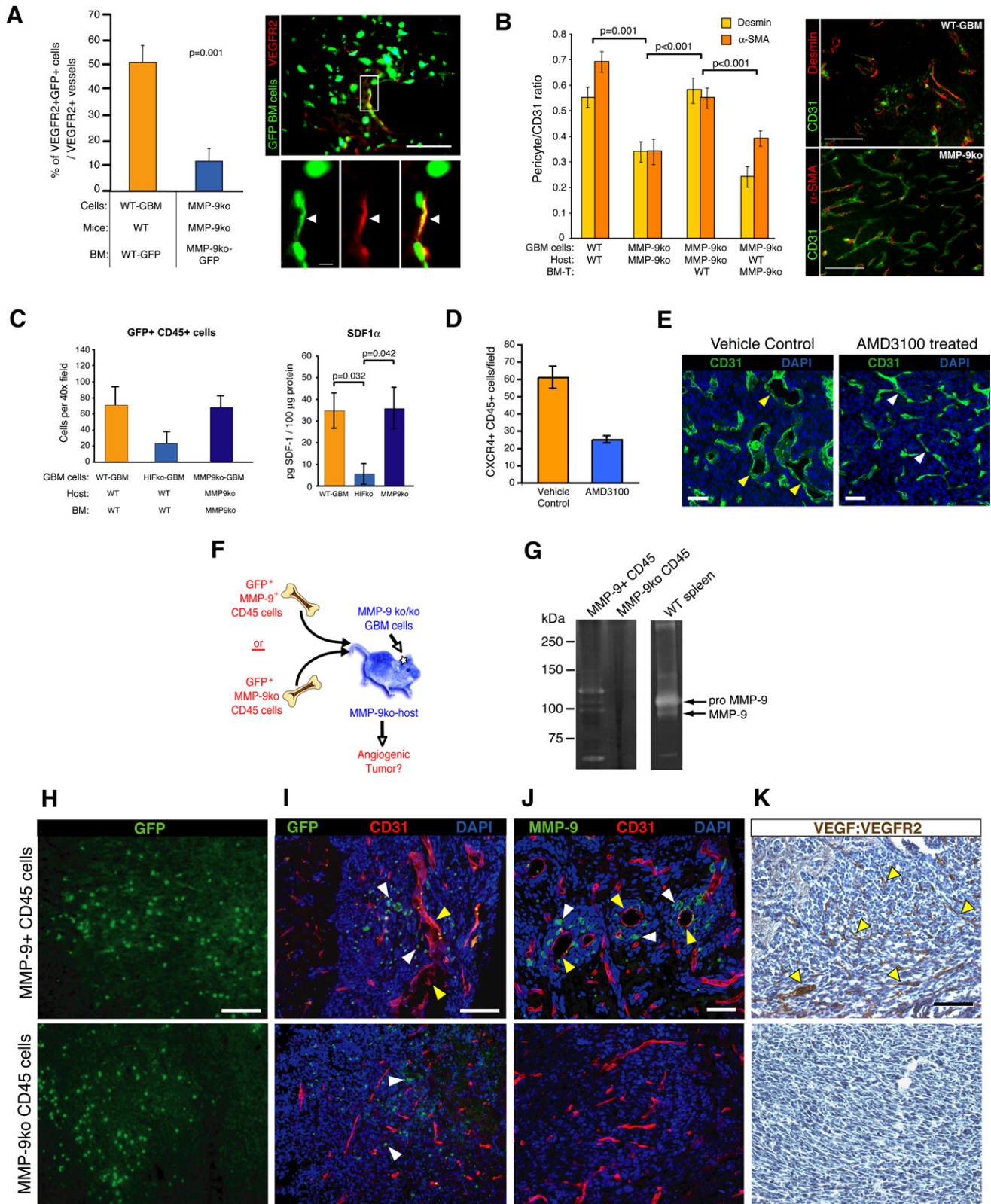
Figure 5. CD45+ MMP-9+ BMDCs Are Sufficient to Initiate Angiogenesis in GBM
(A) Wild-type mice or MMP-9ko mice, reconstituted with bone marrow from actin-GFP wild-type or MMP-9ko mice, respectively, were injected with WT-GBM or MMP-9ko GBM cells. MMP-9ko GBM revealed a 4- to 5-fold reduction of VEGFR2+ (red) GFP+ (green) EPCs. Cohorts of five mice per group were used.

vascular remodeling in GBMs (Figure 7). HIF1 not only induces VEGF transcription in GBM, but also increases VEGF activity by recruiting CD45+ BMDC that carry and secrete the metalloproteinase MMP-9 to the tumor site, which in turn makes sequestered VEGF bioavailable for its receptor VEGFR2 (Figure 7). We found that MMP-9 was expressed in all the CD45+ monocytic cell types that have been implicated in angiogenesis, including TEMs, VEGFR1+ hemangiocytes, CD11b+ immature myeloid cells, and TAMs. These data suggest that MMP-9 is a critical molecule for the different CD45+ vascular modulating cells to promote angiogenesis. Our result that MMP-9 expressed by CD45+ cells is necessary and sufficient to drive neovascularization supports this conclusion. We noticed that most VEGFR1+ hemangiocytes and TEMs express MMP-9, which may explain why inhibition of these cells impairs neovascularization, although these cell types constitute less than 10% of the CD45+ population (De Palma et al., 2005; Jin et al., 2006; Rafii et al., 2002). Importantly, our study indicates that tumors need to have a threshold of MMP-9 levels to initiate the angiogenic switch.

We further revealed that not only the recruitment of EPCs, but also that of PPC into tumors, depended on HIF1 activity and was regulated by MMP-9. PPCs are critical for supplying tumor vessels with sufficient pericytes and for supporting vessel stability and endothelial cell survival in tumors (Song et al., 2005).

In contrast to several other studies (Jin et al., 2006; Jodele et al., 2005), we did not observe that MMP-9 impacted the recruitment of CD45+ BMDCs, although HIF1 activity did. One explanation for the different recruitment mechanisms may lie in distinct signaling circuits that drive recruitment of the respective BMDCs. In our study, HIF1-induced VEGF and SDF1α in tumor cells dictated the influx of BMDCs. While VEGF is an important factor for the activation of MMP-9 in the bone marrow and subsequent mobilization of vascular progenitor cells (Hattori et al., 2001), SDF1α may be crucial for retaining CD45+ populations within the tumor (Grunewald et al., 2006) (Petit et al., 2007). This may explain why tumors growing in a completely MMP-9-deficient environment, which has comparably high SDF1α levels, have reduced numbers of EPCs and PPCs that are recruited in response to VEGF activity but unaltered levels of CD45+ cells. HIFko tumors exhibited reduced levels of both SDF1α and VEGF and recruited fewer vascular progenitors and CD45+ modulatory cells. We conclude that, while HIF1 induces vascular progenitors and monocytic vascular modulatory cells, it is the monocytic population that is sufficient to drive neovascularization. While these studies were performed in an immunocompromised system, it is noteworthy that BMDC influx was found to be independent of the host's immune competence status in another orthotopic glioma model (Joanna Philips and Z.W., unpublished data).

## VEGF Regulates Invasiveness of Tumor Cells

Increased bioavailability of VEGF due to influx of MMP-9 expressing CD45+ cells not only induced angiogenesis, but also regulated tumor cell invasiveness. VEGF prevented tumor cell migration along blood vessels, but appeared to promote tumor cell infiltration into the brain parenchyma. This action of VEGF as a brake on perivascular GBM tumor cell migration is surprising and novel. We observed enhanced invasiveness in the GBM model when VEGF-dependent neovascularization was blocked by genetically deleting the angiogenic regulators VEGF, HIF1α or MMP-9 (Blouw et al., 2003 and present paper). Tumor cells dispersed deep into the brain parenchyma by using blood vessels as a freeway system for perivascular tumor invasion. This invasive mode is distinct from single cells infiltrating into the brain parenchyma and suggests differing mechanisms, also supported by the fact that perivascular tumor cell invasion is independent of MMP-9 and MMP-2 (Du et al., 2008). In contrast, infiltrating tumor cells at the invading edge of WT-GBM expressed MMP-9, suggestive of MMP-9 as a direct regulator in tumor cell infiltration. Further support for this hypothesis stems from in vitro studies showing that decreasing MMP-9 in GBM cells reduced their invasive capacity (Hu et al., 2007; Lakka et al., 2004). How is perivascular invasion regulated by VEGF? Our observation that both MMP-9ko and HIFko GBM are well vascularized with a rather normal and more functional vasculature than the distorted and sparse tumor vasculature of WT-GBMs suggests that it is unlikely that tumor cells move out due to insufficient oxygen and nutrient intake (Blouw et al., 2003). Alternatively, VEGF could directly signal through tumor cells and thereby affect their migration behavior. Congruent with the observation that a variety of tumors express VEGFR1 or -2 and their neuropilin coreceptors (Lesslie et al., 2006; Rao, 2003), we found that GBM cells express VEGFR1 and -2 and neuropilin 1 and 2 and that addition of VEGF to tumor cells or the generation of tumor cells that ectopically express high levels of VEGF-164 reduced the migration capacity of tumor cells. Whether VEGFR1 and -2 or neuropilins play a prominent role in regulating tumor cell migration remains to be determined.

---

(B) Tumor sections of the groups described in Figures 4A–4D were analyzed for the presence of pericytes on tumor vessels as detected by desmin (red) and α-SMA-staining (red) and quantified using the ratios of red-labeled pericytes to green-labeled tumor vessels (anti-CD31 staining).

(C) GFP+CD45+ cells were substantially reduced in HIFko GBM when compared to WT-GBM or MMP-9ko GBM. ELISA assay. SDF1α levels were assessed in tumor lysates of WT-GBM, HIFko GBM, and MMP-9ko GBM. Intratumoral SDF1α levels were lower in HIFko GBM than WT-GBM or MMP-9ko GBM (n = 3 to 4 per group).

(D) WT-GBM mice were treated with the CXCR4 inhibitor AMD3100 or with vehicle control for 2 weeks. AMD3100-treated tumors exhibited a 2- to 3-fold decrease in CXCR4+ CD45+ cells compared to controls.

(E) AMD3100-treated mice demonstrated slimmer and more normalized tumor vessels, while control mice were hyperdilated and tortuous. Scale bars, 50 μm.

(F) Experimental design for assessing functional significance of MMP-9 in CD45+ BMDCs in initiating tumor angiogenesis.

(G) Zymogram analysis of MMP-9ko GBMs from mice that either received GFP+MMP-9+ or GFP+MMP-9ko CD45+ cells. A spleen lysate from a wild-type animal served as a positive control for MMP-9.

(H) Comparable numbers of i.v. injected MMP-9+ or MMP-9ko GFP+CD45+ cells were recruited to the tumor site. All scale bars, 50 μm.

(I) MMP-9ko GBMs that contained MMP-9+CD45+GFP+ cells (white arrowheads) exhibited irregularly shaped and hyperdilated vessels (yellow arrowheads) whereas MMP-9ko GBMs that recruited MMP9koCD45+GFP+ cells (white arrowheads) did not.

(J) MMP-9+ cells (white arrowheads) were preferentially located around hyperdilated vessels (yellow arrowheads).

(K) The vasculature of tumors containing MMP-9+CD45+GFP+ cells became activated (indicated by the presence of VEGF:VEGFR2 complexes on endothelial cells). MMP-9ko tumors that recruited MMP-9ko CD45+ cells did not show VEGF:VEGFR2 complex formations. All error bars indicate ± SEM.
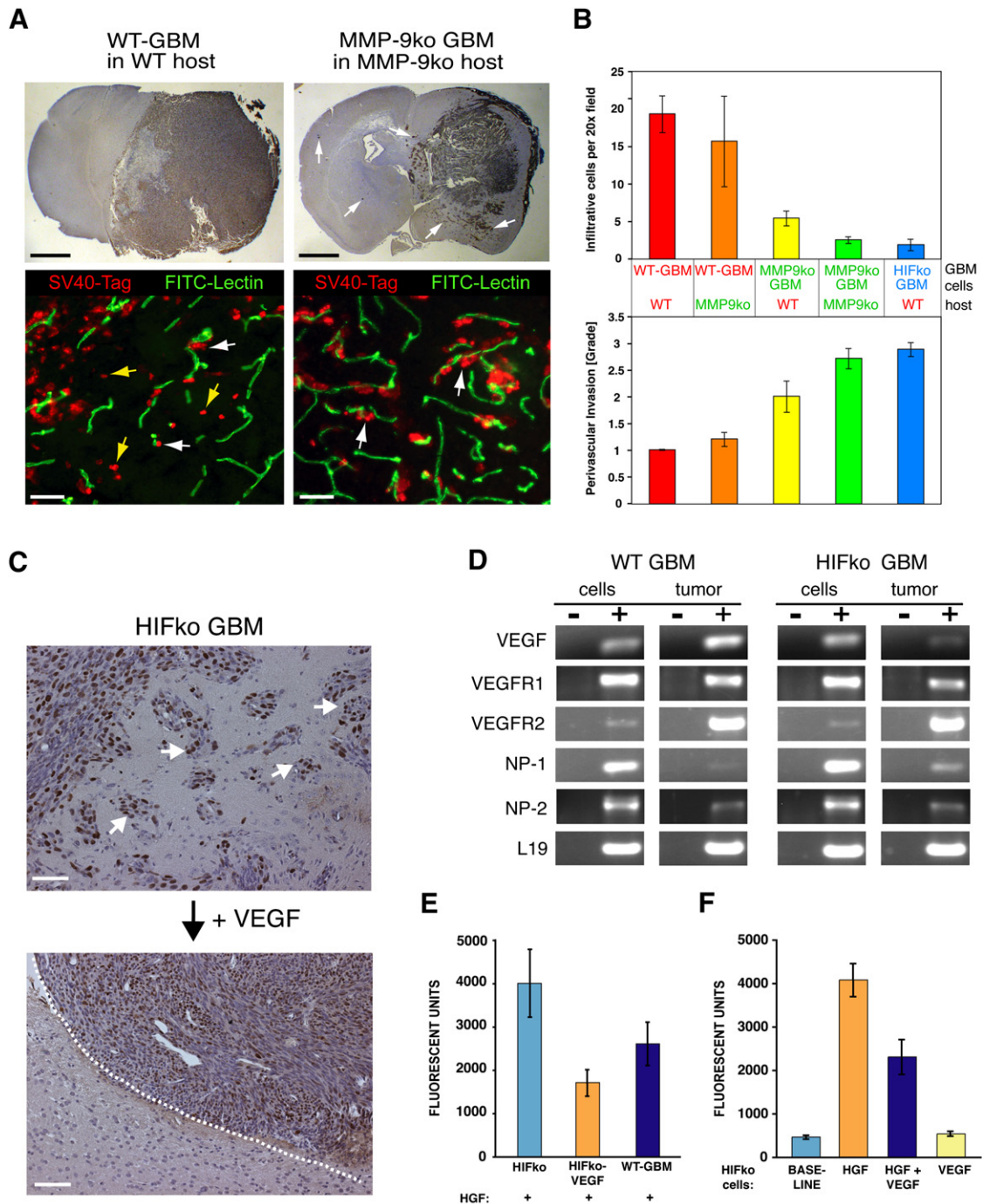
**Figure 6. VEGF Directly Inhibits Perivascular Tumor Invasion**

(A) Fluorescent detection of tumor cells (anti-SV40-Tag antibody; red) and the vasculature (FITC-lectin; green). WT-GBM cells infiltrated as single cells into the brain parenchyma without associating with blood vessels (yellow arrows) or invaded alongside blood vessels (perivascular invasion) in the brain (white arrows). MMP-9ko GBMs were predominantly perivascular invasive. Black bar, 1.4 mm. White bar, 50 μm.

(B) Infiltrative and perivascular invasive modes of GBMs in different tumor cell/host combinations were quantified by immunohistochemical analysis on tumor sections as in Figure 6A. Infiltrative cells were counted as cells in the brain without vessel association, whereas perivascular invasiveness of tumor cells was graded from 0–3, where 1 indicates minimal distant spread of tumor cells and 3 indicates substantial and marked distant spread. Error bars indicate ± SD.

(C) HIFko GBM were stably transduced with a retrovirus expressing VEGF-164. While HIFko GBMs were perivascular invasive (white arrows), HIFko GBMs over-expressing VEGF exhibited a smooth tumor border (dotted line) and did not invade. Scale bars, 50 μm.

(D) RT-PCR analysis revealed that both WT-GBM and HIFko GBM express VEGFR1, 2 and neuropilin1, 2.

(E and F) Boyden Chamber invasion assay. (E) Ectopic expression of VEGF in HIFko GBM or (F) addition of recombinant VEGF to HIFko GBM cells reduced tumor cell migration by about 50% in response to HGF. VEGF alone had no effect. Error bars indicate ± SEM.
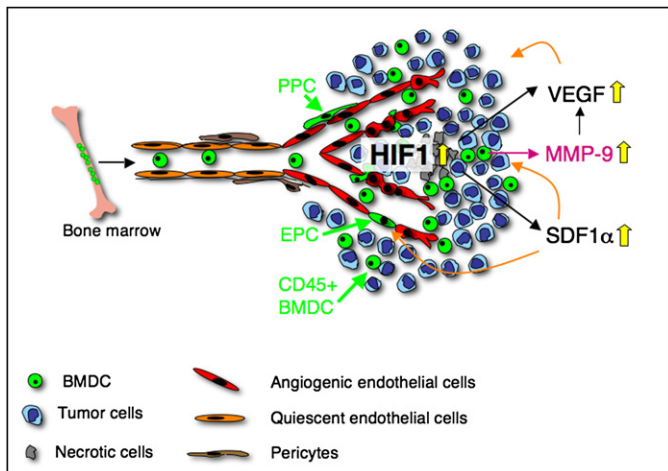
**Figure 7. HIF-1 Is a Critical Regulator of BMDC Recruitment in Tumors**

Hypoxia in tumors increases HIF1, which, partly by inducing VEGF and SDF1α in tumor cells, recruits BMDC including EPC, PPC, and CD45+ monocytic vascular modulatory cells to endorse vascular remodeling in glioblastomas. SDF1α serves as a retention factor of CXCR4+ vascular progenitor and monocytic BMDC in GBM. HIF1 not only induces VEGF transcription in GBM, but also increases VEGF activity by recruiting CD45+ BMDC that carry and secrete MMP-9 to the tumor site, which in turn makes sequestered VEGF bioavailable for its receptor VEGFR2.

## Clinical Implications

The observation that hypoxia is a driving force in BMDC-dependent neovascularization of tumors also has clinical implications. Hypoxia occurs not only in certain tumor types during progression, but also in tumors that undergo antiangiogenic therapy due to vessel regression. Therefore, combinatorial treatment modalities blocking both proangiogenic receptor tyrosine kinase signaling circuits and the recruitment of vascular progenitor and modulatory BMDCs may reveal synergistic effects and survival benefit. Similarly, GBM patients undergo daily radiation after surgery to kill as many remaining tumor cells as possible. This treatment might be a double-edged sword because radiation also mobilizes bone marrow cells into the blood stream (Heissig et al., 2005) that could account for the fast tumor relapse that often occurs in GBM patients. Our results suggest that radiation should occur in combination with CXCR4 inhibitors or other BMDC-targeting agents to block BMDC recruitment and subsequent neovascularization and regrowth of tumors.

Our observation that tumor cells increase their perivascular invasiveness in the absence of VEGF activity was also found in a human GBM xenograft model treated with the VEGF inhibitor SU5416 (Rubenstein et al., 2000). Moreover, a proinvasive adaptation has been inferred from MRI imaging in a subset of GBM patients that had developed multifocal recurrence of tumors during the course of anti-VEGF (bevacuzimab) therapy (M. Prados and N. Butowski, personal communication). These data implicate that GBMs impaired in angiogenesis, for example, when targeted with anti-VEGF agents, can evade from their inability to induce angiogenesis by becoming more invasive. It will, therefore, be instrumental to identify pathways that simultaneously block perivascular invasion and angiogenesis to improve current antiangiogenic therapeutic implications in GBM and potentially other tumors.

## EXPERIMENTAL PROCEDURES

### Generation of WT-GBM, HIFko GBM, HIFko MMP-9+, and MMP9ko GBM Transformed Mouse Astrocytes

Generation of WT-GBM and HIFko GBM transformed mouse astrocytes has been described previously (Blouw et al., 2003). MMP-9ko GBM cells were generated from MMP-9ko/ko FvBN Ragko mice using the same approach. HIFko

MMP-9+ cells overexpressing MMP-9 were generated by retroviral transduction of HIFko GBM cells with an autoactivating form of murine *MMP-9* (kind gift from Dr. Elaine Raines) (Gough et al., 2006). HIFko Mock control cells were generated with an empty retroviral construct. All animal housing, care, and experiments were performed in accordance with the UCSF institutional and national guidelines and regulations governing care of laboratory mice.

### Bone Marrow Transplantation

Bone marrow was harvested from 6- to 8-week-old β-actin-EGFP Rag1ko or Rag1ko MMP-9ko/ko mice by flushing the femurs and tibias with 2% FBS in phosphate-buffered saline (PBS). Cells ($2 \times 10^6$) were intravenously (i.v.) injected through the tail vein of lethally irradiated (10 Gy) recipient mice. Tumor cell implantation was performed intracranially (i.c.) 4 weeks later.

### Intracranial Implantation of Astrocytomas

Six- to eight-week-old FvBN Rag1ko or Rag1ko/MMP-9ko mice were implanted i.c. as described previously (Blouw et al., 2003) with 2.5 μl of $0.7 \times 10^6$ WT-GBM, HIFko, MMP-9ko, or HIFko MMP-9+ GBM cells. All mice were sacrificed 14 to 21 days after tumor cell implantation. Tumors were isolated from the brain and prepared for flow cytometric analyses, immunohistochemical staining, or protein and RNA isolation as described below. All implantation experiments were repeated up to three times for a total of up to ten mice per group.

### AMD3100 Treatment

Ten FvBN Rag1ko mice injected i.c. with WT-GBM cells were randomized into two cohorts for AMD3100 treatment or control treatment. Beginning 3 days prior to tumor cell implantation, AMD3100 (Sigma) or PBS was subcutaneously (s.c.) administered at 1.25 mg/kg twice daily in the right and left flank for 2 weeks, with the exception of single doses on weekends. Experiments were performed four times (n = 20 treated mice and 20 control mice).

### Isolation of GFP+ CD45+ Bone Marrow Cells

CD45+ cells were isolated from the bone marrow of wild-type β-actin-EGFP Ragko mice or MMP9 ko/ko β-actin-EGFP Ragko mice using a biotinylated rat antibody against murine CD45 and the EasySep Biotin Selection Kit (StemCell Technologies). Isolated GFP+ CD45+ bone marrow cells ($2 \times 10^6$) were injected i.v. every 3 to 4 days for a total of four injections over 2 weeks into MMP-9 ko/ko mice that had been implanted with MMP9ko GBM cells a day prior to onset of CD45 cell injections. Experiments were repeated four times with four to five mice per group.

### Flow Cytometry

GBMs from GFP bone marrow-transplanted mice were prepared as single cell suspensions as described (Song et al., 2005) and stained with the following antibodies: FITC-, APC-, PE-, or biotin-conjugated rat antibodies against murine CD45, Tie-2, F4/80, VEGFR2, and PDGFRβ (eBioscience, San Diego, CA), CXCR4 and Sca-1 (BD Biosciences), VEGFR1 clone MF1 (Imclone Systems, New York, NY), and a goat antibody against murine VE-cadherin (Santa Cruz Biotechnology, Santa Cruz, CA). CD45+ populations were analyzed for expression of Tie-2, F4/80, CD11b, and VEGFR1. EPCs were identified by double-positivity for VEGFR2 and VE-cadherin. PPCs were detected by double

staining of PDGFRβ and Sca-1. Stained cells were measured on a FACsAria flow cytometer (Becton Dickinson, NJ) and analyzed using FlowJo software (Tree Star Inc., Ashland, OR). Experiments were repeated up to five times, with two to three independent tumor samples for each combination of markers analyzed.

### Tissue Preparation
To prepare tissues for immunohistochemical staining, mice were anesthetized and cardiac-perfused with PBS and 4% paraformaldehyde (PFA) and embedded into paraffin or OCT.

### Immunohistochemistry
Frozen or paraffin sections were used for immunohistochemical analysis. To visualize the vasculature, mice were intravenously injected with FITC- or Rhodamine-conjugated lectin prior to PBS/PFA heart perfusion and fixation. Vessel imaging on frozen sections was enhanced by staining sections with a 1:100 dilution of a rat anti-mouse CD31 antibody (BD Biosciences). BMDC populations were analyzed on frozen sections by staining with 1:500 dilutions of rat anti-mouse CD45 and CD11b (BD Biosciences), 1:100 Tie-2 (eBioscience), 1:500 F4/80 (Serotec, Raleigh, NC), and 1:150 VEGFR1 clone MF1 (Imclone Systems) antibodies. MMP-9 was detected with a 1:500 dilution of a rabbit anti-MMP-9 antibody (Behrendtsen and Werb, 1997). Staining of SDF1α was performed on frozen sections using a rabbit anti-SDF1α antibody (1:100, Cell Sciences, Canton, MA). VEGFR2 staining was performed on paraffin-embedded sections with a goat anti-mouse VEGFR2 antibody (1:50, R&D Systems). VEGF-VEGFR2 complex was visualized in frozen sections with a mouse monoclonal antibody Gv39M (1:50, EastCoast Bio, North Berwick, ME). Pericytes were identified with a mouse anti-human desmin (1:100, DAKO Corp.) and mouse anti-human alpha smooth muscle actin (1:500, DAKO Corp.). For fluorescent visualization of antibody reactions, secondary antibodies were labeled with the fluorochromes AlexaFluor488, AlexaFluor594, or AlexaFluor633 (1:200; Molecular Probes, Eugene, OR), while nuclei were detected with DAPI. Photomicrographs were taken with a Zeiss Axiovert 2 microscope using Openlab 3 software (Improvision, Lexington, MA) or a Zeiss LSM 510 laser scanning confocal microscope using Zeiss LSM Image Browser software.

### Quantification of Pericyte Coverage
Fluorescent images of tumor sections were collected on a Zeiss Axioskop 2 with 20× Plan Neofluar lenses and a Zeiss Axiocam color CCD. Red, green, and blue staining was quantitatively evaluated using ImageJ v1.34 software (NIH). The total area of CD31, desmin, or αSMA staining was obtained. The fraction of pericyte coverage was calculated as the ratio of the area of desmin or α-SMA staining (red) to the area of CD31 staining (green). For desmin staining, 8 to 17 tumor sections per group were evaluated. For α-SMA staining, four to nine tumor sections per group were evaluated.

### Substrate Zymography
Tumors were trimmed out of the brain and homogenized (1:3 w/v) in RIPA lysis buffer and analyzed by gelatin zymography as described previously (Bergers et al., 2000). EDTA (20 mM) was added to the gelatinase buffer overnight to confirm that the proteases were metalloproteinases.

### RNA Isolation, RT-PCR, and Real-Time PCR Analysis
RNA isolation was performed on cell cultures or whole tissue with TRIzol Reagent (Invitrogen). First-strand cDNA was generated using the SuperScript II First Strand Synthesis System (Invitrogen). Primer sequences are listed in Figure S4.

### Nonradioactive In Situ Hybridization
Nonradioactive in situ hybridization of RGS-5 was performed as published previously (Berger et al., 2005).

### Extraction of VEGF and Immunoblotting
Supernatants of 70% confluent WT GBM and HIFko GBM cells were collected for 20 hr in serum-free medium and Insulin-Transferrin-Selenium and concentrated 50-fold in a microconcentrator (Millipore). Cell extracts were prepared by gently scraping off cells in 1× calcium and magnesium-free PBS followed by extraction in RIPA buffer containing 1× protease inhibitors (Roche). ECM proteins were extracted after complete removal of cells from cell culture dishes in RIPA buffer as described (Park et al., 1993). Western blot analysis was performed with 15 μg protein for cell supernatants and 150 μg for ECM and cell extracts and probed with a goat anti-mouse VEGF antibody (1:200; R&D Systems, Minneapolis, MN) or an anti-mouse tubulin antibody (1:5000; Calbiochem) as loading control. VEGF and tubulin was quantified by densitometry using Image J 1.38.

### SDF-1α and VEGF ELISA
SDF-1α or VEGF levels were determined by ELISA in WT GBM, HIFko GBM, MMP-9ko GBM, and HIFko MMP9+ astrocytes or from dissected tumors or blood of either WT GBM, MMP-9ko GBM, or HIFko GBM mice using the Quantikine mouse SDF-1α kit and mouse VEGF kit (R&D Systems).

### Invasion Assay
Fifty percent confluent HIFko or WT-GBM or HIFko-VEGF astrocytoma cells were switched to serum-free DMEM medium containing no VEGF or VEGF (50 ng/ml) for 18 hr, trypsinized, and seeded at $1 \times 10^5$ cells/well in 24-well matrigel plates (Fluoroblock; BD Falcon) in medium containing 40ng/ml HGF with either no VEGF or 100 ng/ml VEGF in the lower chamber. Invasion was assayed after 20 hr using Calcein AM as substrate on a cytoflour (excitation 485/20; emission 530/35; 50% gain).

### Statistical Analysis
All experiments were repeated two to four times. Statistical analyses were performed with the Kruskal-Wallis H test or the two-tailed Student's t test to determine statistical significance, followed by a Mann-Whitney U test for pairwise comparison. p values (exact significance) of <0.05 were considered statistically significant. Results are expressed as mean ± SEM or SD as indicated. Kaplan-Meier curves and the log-rank test were used to compare survival times among the groups. All calculations were performed using SPSS v11.0 (SPSS Inc., Chicago, IL).

### SUPPLEMENTAL DATA

The Supplemental Data include four supplemental figures and can be found with this article online at http://www.cancercell.org/cgi/content/full/13/3/206/DC1/.

### REFERENCES

Abounader, R., and Laterra, J. (2005). Scatter factor/hepatocyte growth factor in brain tumor growth and angiogenesis. Neuro-Oncol. 7, 436–451.

Aghi, M., and Chiocca, E.A. (2005). Contribution of bone marrow-derived cells to blood vessels in ischemic tissues and tumors. Mol. Ther. 12, 994–1005.

Aghi, M., Cohen, K.S., Klein, R.J., Scadden, D.T., and Chiocca, E.A. (2006). Tumor stromal-derived factor-1 recruits vascular progenitors to mitotic neovasculature, where microenvironment influences their differentiated phenotypes. Cancer Res. 66, 9054–9064.

Behrendtsen, O., and Werb, Z. (1997). Metalloproteinases regulate parietal endoderm differentiating and migrating in cultured mouse embryos. Dev. Dyn. 208, 255–265.

Berger, M., Bergers, G., Arnold, B., Hammerling, G.J., and Ganss, R. (2005). Regulator of G-protein signaling-5 induction in pericytes coincides with active vessel remodeling during neovascularization. Blood 105, 1094–1101.

Bergers, G., Brekken, R., McMahon, J., Vu, T.H., Itoh, T., Tamaki, K., Tanzawa, K., Thorpe, P., Itohara, S., Werb, Z., and Hanahan, D. (2000). Matrix Metallo-proteinase-9 triggers the angiogenic switch during carcinogenesis. Nat. Cell Biol. 2, 737–744.

Blouw, B., Song, H., Tihan, T., Bosze, J., Ferrara, N., Gerber, H.P., Johnson, R.S., and Bergers, G. (2003). The hypoxic response of tumors is dependent on their microenvironment. Cancer Cell 4, 133–146.

Bondjers, C., Kalen, M., Hellstrom, M., Scheidl, S.J., Abramsson, A., Renner, O., Lindahl, P., Cho, H., Kehrl, J., and Betsholtz, C. (2003). Transcription pro-filing of platelet-derived growth factor-B-deficient mouse embryos identifies RGS5 as a novel marker for pericytes and vascular smooth muscle cells. Am. J. Pathol. 162, 721–729.

Brekken, R.A., Overholser, J.P., Stastny, V.A., Waltenberger, J., Minna, J.D., and Thorpe, P.E. (2000). Selective inhibition of vascular endothelial growth fac-tor (VEGF) receptor 2 (KDR/Flk-1) activity by a monoclonal anti-VEGF antibody blocks tumor growth in mice. Cancer Res. 60, 5117–5124.

Calvani, M., Rapisarda, A., Uranchimeg, B., Shoemaker, R.H., and Melillo, G. (2006). Hypoxic induction of an HIF-1alpha-dependent bFGF autocrine loop drives angiogenesis in human endothelial cells. Blood 107, 2705–2712.

Ceradini, D.J., Kulkarni, A.R., Callaghan, M.J., Tepper, O.M., Bastidas, N., Kleinman, M.E., Capla, J.M., Galiano, R.D., Levine, J.P., and Gurtner, G.C. (2004). Progenitor cell trafficking is regulated by hypoxic gradients through HIF-1 induction of SDF-1. Nat. Med. 10, 858–864.

De Falco, E., Porcelli, D., Torella, A.R., Straino, S., Iachininoto, M.G., Orlandi, A., Truffa, S., Biglioli, P., Napolitano, M., Capogrossi, M.C., and Pesce, M. (2004). SDF-1 involvement in endothelial phenotype and ischemia-induced re-cruitment of bone marrow progenitor cells. Blood 104, 3472–3482.

De Palma, M., Venneri, M.A., Galli, R., Sergi, L.S., Politi, L.S., Sampaolesi, M., and Naldini, L. (2005). Tie2 identifies a hematopoietic lineage of proangiogenic monocytes required for tumor vessel formation and a mesenchymal popula-tion of pericyte progenitors. Cancer Cell 8, 211–226.

Du, R., Petritsch, C., Lu, K., Liu, P., Ganss, R., Song, H., VandenBerg, S., and Bergers, G. (2008). Matrix Metalloproteinase-2 regulates vascular patterning and growth affecting tumor cell survival and invasion in GBM. Neuro-Oncol., in press.

Dvorak, H.F. (2000). VPF/VEGF and the angiogenic response. Semin. Perina-tol. 24, 75–78.

Eckerich, C., Zapf, S., Fillbrandt, R., Loges, S., Westphal, M., and Lamszus, K. (2007). Hypoxia can induce c-Met expression in glioma cells and enhance SF/HGF-induced cell migration. Int. J. Cancer 121, 276–283.

Gerhardt, H., and Betsholtz, C. (2003). Endothelial-pericyte interactions in an-giogenesis. Cell Tissue Res. 314, 15–23.

Giaccia, A.J., Simon, M.C., and Johnson, R. (2004). The biology of hypoxia: The role of oxygen sensing in development, normal function, and disease. Genes Dev. 18, 2183–2194.

Gough, P.J., Gomez, I.G., Wille, P.T., and Raines, E.W. (2006). Macrophage expression of active MMP-9 induces acute plaque disruption in apoE-deficient mice. J. Clin. Invest. 116, 59–69.

Grunewald, M., Avraham, I., Dor, Y., Bachar-Lustig, E., Itin, A., Jung, S., Chimenti, S., Landsman, L., Abramovitch, R., and Keshet, E. (2006). VEGF-in-duced adult neovascularization: Recruitment, retention, and role of accessory cells. Cell 124, 175–189.

Hattori, K., Dias, S., Heissig, B., Hackett, N.R., Lyden, D., Tateno, M., Hicklin, D.J., Zhu, Z., Witte, L., Crystal, R.G., et al. (2001). Vascular endothelial growth factor and angiopoietin-1 stimulate postnatal hematopoiesis by recruitment of vasculogenic and hematopoietic stem cells. J. Exp. Med. 193, 1005–1014.

Hattori, K., Heissig, B., and Rafii, S. (2003). The regulation of hematopoietic stem cell and progenitor mobilization by chemokine SDF-1. Leuk. Lymphoma 44, 575–582.

Hattori, K., Heissig, B., Wu, Y., Dias, S., Tejada, R., Ferris, B., Hicklin, D.J., Zhu, Z., Bohlen, P., Witte, L., et al. (2002). Placental growth factor reconstitutes he-matopoiesis by recruiting VEGFR1(+) stem cells from bone-marrow microen-vironment. Nat. Med. 8, 841–849.

Heissig, B., Hattori, K., Dias, S., Friedrich, M., Ferris, B., Hackett, N.R., Crystal, R.G., Besmer, P., Lyden, D., Moore, M.A., et al. (2002). Recruitment of stem and progenitor cells from the bone marrow niche requires MMP-9 mediated re-lease of kit-ligand. Cell 109, 625–637.

Heissig, B., Rafii, S., Akiyama, H., Ohki, Y., Sato, Y., Rafael, T., Zhu, Z., Hicklin, D.J., Okumura, K., Ogawa, H., et al. (2005). Low-dose irradiation promotes tis-sue revascularization through VEGF release from mast cells and MMP-9-me-diated progenitor cell mobilization. J. Exp. Med. 202, 739–750.

Holash, J., Maisonpierre, P.C., Compton, D., Boland, P., Alexander, C.R., Zag-zag, D., Yancopoulos, G.D., and Wiegand, S.J. (1999). Vessel cooption, re-gression, and growth in tumors mediated by angiopoietins and VEGF. Science 284, 1994–1998.

Hormigo, A., Gu, B., Karimi, S., Riedel, E., Panageas, K.S., Edgar, M.A., Tan-war, M.K., Rao, J.S., Fleisher, M., DeAngelis, L.M., and Holland, E.C. (2006). YKL-40 and matrix metalloproteinase-9 as potential serum biomarkers for pa-tients with high-grade gliomas. Clin. Cancer Res. 12, 5698–5704.

Hu, B., Guo, P., Bar-Joseph, I., Imanishi, Y., Jarzynka, M.J., Bogler, O., Mikkel-sen, T., Hirose, T., Nishikawa, R., and Cheng, S.Y. (2007). Neuropilin-1 pro-motes human glioma progression through potentiating the activity of the HGF/SF autocrine pathway. Oncogene 26, 5577–5586.

Jin, D.K., Shido, K., Kopp, H.G., Petit, I., Shmelkov, S.V., Young, L.M., Hooper, A.T., Amano, H., Avecilla, S.T., Heissig, B., et al. (2006). Cytokine-mediated deployment of SDF-1 induces revascularization through recruitment of CXCR4+ hemangiocytes. Nat. Med. 12, 557–567.

Jodele, S., Chantrain, C.F., Blavier, L., Lutzko, C., Crooks, G.M., Shimada, H., Coussens, L.M., and Declerck, Y.A. (2005). The contribution of bone marrow-derived cells to the tumor vasculature in neuroblastoma is matrix metallopro-teinase-9 dependent. Cancer Res. 65, 3200–3208.

Kopp, H.G., Ramos, C.A., and Rafii, S. (2006). Contribution of endothelial pro-genitors and proangiogenic hematopoietic cells to vascularization of tumor and ischemic tissue. Curr. Opin. Hematol. 13, 175–181.

Kunishio, K., Okada, M., Matsumoto, Y., and Nagao, S. (2003). Matrix metal-loproteinase-2 and −9 expression in astrocytic tumors. Brain Tumor Pathol. 20, 39–45.

Lakka, S.S., Gondi, C.S., Yanamandra, N., Olivero, W.C., Dinh, D.H., Gujrati, M., and Rao, J.S. (2004). Inhibition of cathepsin B and MMP-9 gene expression in glioblastoma cell line via RNA interference reduces tumor cell invasion, tumor growth and angiogenesis. Oncogene 23, 4681–4689.

Lesslie, D.P., Summy, J.M., Parikh, N.U., Fan, F., Trevino, J.G., Sawyer, T.K., Metcalf, C.A., Shakespeare, W.C., Hicklin, D.J., Ellis, L.M., and Gallick, G.E. (2006). Vascular endothelial growth factor receptor-1 mediates migration of human colorectal carcinoma cells by activation of Src family kinases. Br. J. Cancer 94, 1710–1717.

Li, B., Sharpe, E.E., Maupin, A.B., Teleron, A.A., Pyle, A.L., Carmeliet, P., and Young, P.P. (2006). VEGF and PlGF promote adult vasculogenesis by enhanc-ing EPC recruitment and vessel formation at the site of tumor neovasculariza-tion. FASEB J. 20, 1495–1497.

Liao, D., Corle, C., Seagroves, T.N., and Johnson, R.S. (2007). Hypoxia-induc-ible factor-1alpha is a key regulator of metastasis in a transgenic model of cancer initiation and progression. Cancer Res. 67, 563–572.

Lin, E.Y., Li, J.F., Gnatovskiy, L., Deng, Y., Zhu, L., Grzesik, D.A., Qian, H., Xue, X.N., and Pollard, J.W. (2006). Macrophages regulate the angiogenic switch in a mouse model of breast cancer. Cancer Res. 66, 11238–11246.

Lofstedt, T., Fredlund, E., Holmquist-Mengelbier, L., Pietras, A., Ovenberger, M., Poellinger, L., and Pahlman, S. (2007). Hypoxia inducible factor-2alpha in cancer. Cell Cycle 6, 919–926.

Lyden, D., Hattori, K., Dias, S., Costa, C., Blaikie, P., Butros, L., Chadburn, A., Heissig, B., Marks, W., Witte, L., et al. (2001). Impaired recruitment of bone-marrow-derived endothelial and hematopoietic precursor cells blocks tumor angiogenesis and growth. Nat. Med. 7, 1194–1201.

Maxwell, P.H., Dachs, G.U., Gleadle, J.M., Nicholls, L.G., Harris, A.L., Stratford, I.J., Hankinson, O., Pugh, C.W., and Ratcliffe, P.J. (1997). Hypoxia-inducible factor-1 modulates gene expression in solid tumors and influences both angiogenesis and tumor growth. Proc. Natl. Acad. Sci. USA 94, 8104–8109.

Nozawa, H., Chiu, C., and Hanahan, D. (2006). Infiltrating neutrophils mediate the initial angiogenic switch in a mouse model of multistage carcinogenesis. Proc. Natl. Acad. Sci. USA 103, 12493–12498.

Okuyama, H., Krishnamachary, B., Zhou, Y.F., Nagasawa, H., Bosch-Marce, M., and Semenza, G.L. (2006). Expression of vascular endothelial growth factor receptor 1 in bone marrow-derived mesenchymal cells is dependent on hypoxia-inducible factor 1. J. Biol. Chem. 281, 15554–15563.

Page-McCaw, A., Ewald, A.J., and Werb, Z. (2007). Matrix metalloproteinases and the regulation of tissue remodelling. Nat. Rev. Mol. Cell Biol. 8, 221–233.

Park, J.E., Keller, G.A., and Ferrara, N. (1993). The vascular endothelial growth factor (VEGF) isoforms: Differential deposition into the subepithelial extracellular matrix and bioactivity of extracellular matrix-bound VEGF. Mol. Biol. Cell 4, 1317–1326.

Petit, I., Jin, D., and Rafii, S. (2007). The SDF-1-CXCR4 signaling pathway: A molecular hub modulating neo-angiogenesis. Trends Immunol. 28, 299–307.

Pollard, J.W. (2004). Tumour-educated macrophages promote tumour progression and metastasis. Nat. Rev. Cancer 4, 71–78.

Rabbany, S.Y., Heissig, B., Hattori, K., and Rafii, S. (2003). Molecular pathways regulating mobilization of marrow-derived stem cells for tissue revascularization. Trends Mol. Med. 9, 109–117.

Rafii, S., Lyden, D., Benezra, R., Hattori, K., and Heissig, B. (2002). Vascular and haematopoietic stem cells: Novel targets for anti-angiogenesis therapy? Nat. Rev. Cancer 2, 826–835.

Rajantie, I., Ilmonen, M., Alminaite, A., Ozerdem, U., Alitalo, K., and Salven, P. (2004). Adult bone marrow-derived cells recruited during angiogenesis comprise precursors for periendothelial vascular mural cells. Blood 104, 2084–2086.

Rao, J.S. (2003). Molecular mechanisms of glioma invasiveness: The role of proteases. Nat. Rev. Cancer 3, 489–501.

Rubenstein, J.L., Kim, J., Ozawa, T., Zhang, M., Westphal, M., Deen, D.F., and Shuman, M.A. (2000). Anti-VEGF antibody treatment of glioblastoma prolongs survival but results in increased vascular cooption. Neoplasia 2, 306–314.

Ryan, H.E., Lo, J., and Johnson, R.S. (1998). HIF-1 alpha is required for solid tumor formation and embryonic vascularization. EMBO J. 17, 3005–3015.

Shweiki, D., Itin, A., Soffer, D., and Keshet, E. (1992). Vascular endothelial growth factor induced by hypoxia may mediate hypoxia-initiated angiogenesis. Nature 359, 843–845.

Song, S., Ewald, A.J., Stallcup, W., Werb, Z., and Bergers, G. (2005). PDGFRbeta+ perivascular progenitor cells in tumours regulate pericyte differentiation and vascular survival. Nat. Cell Biol. 7, 870–879.

Yang, L., DeBusk, L.M., Fukuda, K., Fingleton, B., Green-Jarvis, B., Shyr, Y., Matrisian, L.M., Carbone, D.P., and Lin, P.C. (2004). Expansion of myeloid immune suppressor Gr+CD11b+ cells in tumor-bearing host directly promotes tumor angiogenesis. Cancer Cell 6, 409–421.

Zagzag, D., Zhong, H., Scalzitti, J.M., Laughner, E., Simons, J.W., and Semenza, G.L. (2000). Expression of hypoxia-inducible factor 1alpha in brain tumors: Association with angiogenesis, invasion, and progression. Cancer 88, 2606–2618.